

# Stochastic Search of Molecular Cluster Interaction Energy Surfaces with Coupled Cluster Quality Prediction. The Phenylacetylene Dimer

Matthew A. Addicoat,<sup>†,||</sup> Yoshifumi Nishimura,<sup>†</sup> Takeshi Sato,<sup>‡</sup> Takao Tsuneda,<sup>§</sup> and Stephan Irle<sup>\*,†</sup>

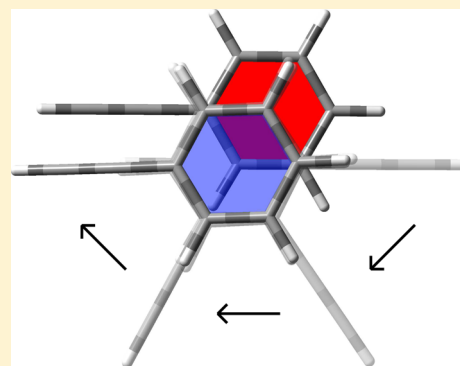
<sup>†</sup>Department of Chemistry, Nagoya University, Furo-cho, Chikusa-ku Nagoya 464-4602, Japan

<sup>‡</sup>Photon Science Center, University of Tokyo, Tokyo 113-8656, Japan

<sup>§</sup>Fuel Cell Nanomaterials Center, University of Yamanashi, Kofu 400-0021, Japan

## S Supporting Information

**ABSTRACT:** We report a stochastic search methodology on the basis of dispersion-augmented density functional theory (DFT), aimed at finding low energy isomers of the phenylacetylene dimer as well as methane and benzene dimers. Stochastic search of the molecular cluster interaction energy surfaces was carried out with the computationally inexpensive dispersion-augmented, third-order self-consistent charge density functional tight-binding (DFTB3-D) method, and energetically low-lying molecular cluster geometries were identified, including several that had previously been optimized at the MP2/cc-pVTZ level of theory and had single point interaction energies evaluated at the coupled-cluster singles, doubles, and perturbative triples (CCSD(T)) level of theory in the complete basis set limit (Maity, S. et al. *Phys. Chem. Chem. Phys.* **2011**, *13*, 16706). In addition, the search procedure identifies several additional low-energy isomers that map a reaction path, rotating one monomer through a full 360° relative to the first. We found that binding energies from long-range corrected functional combined with the local response dispersion correction (LC-BOP+LRD) yields binding energies that are within 1 kJ mol<sup>-1</sup> of the CCSD(T)/CBS results for both  $\pi$ -stacked and CH $\cdots\pi$  structures. In contrast, other functionals and second-order Møller–Plesset perturbation methods favored one binding motif or the other and therefore are not ideal to describe a global potential energy surface.



## INTRODUCTION

Noncovalent and long range interactions play a key role in many physicochemical processes, from determining molecule surface interactions, influencing reaction intermediates,<sup>1</sup> to guiding the 3-dimensional arrangement of polymers, proteins, and nucleic acids. Such interactions are typically small in magnitude, compared to covalent interactions and frequently involve many atoms, and are therefore typically the domain of either high-level calculations<sup>2–5</sup> or have been approximated within molecular mechanics methods.<sup>6,7</sup> However, they may account for more than 50% of isomerization energies in organic compounds,<sup>8</sup> and thus, it is essential to describe them accurately. Recently, several authors<sup>9–24</sup> have focused on accurately describing dispersion effects within DFT, employing approaches including Wannier functions,<sup>25</sup> Random phase Approximation,<sup>26</sup> and various empirical schemes.<sup>13</sup>

Subsequent to these efforts in method development have been a number of studies<sup>27–29</sup> comparing the utility of these methods, or subsets thereof, in accurately describing these weak intermolecular interactions, including van der Waals complexes<sup>30–32</sup> and, specifically,  $\pi$ – $\pi$  and CH $\cdots\pi$  interactions.<sup>33–35</sup>

The benzene dimer<sup>36–38</sup> and substituted analogues,<sup>39</sup> have long been a staple test system for investigating  $\pi$ – $\pi$  interactions. Benzene's larger cousins, naphthalene, and coronene have also been studied using high level *ab initio* calculations, en route to graphitic systems.<sup>40</sup> Studies investigat-

ing Density Functional Theory (DFT) have both focused solely on the benzene dimer<sup>41,42</sup> or employed the benzene dimer as part of a larger test set.<sup>24,43–47</sup> The TPSS functional<sup>48</sup> combined with the  $-D_3$  empirical dispersion correction<sup>13</sup> and the M06-2x<sup>45</sup> functional, which inherently includes dispersion have repeatedly been shown to perform well for noncovalent interactions in general.<sup>29,44,49</sup> In particular, Hobza et al. showed that, overall, density functional methods yielded more consistent results than all bar the most expensive ( $O(N^6)$ ) wave function based methods,<sup>29</sup> providing further motivation to verify the performance of the computationally far less expensive density functional methods. However, the potentially enormous number of orientational isomers in molecular clusters makes a complete search of the molecular interaction potential energy surface impractical even at the DFT level of theory due to the associated computational cost. Here, we report a methodology that is based on approximate DFT, which was used for a global structure search, involving more than 200 stochastically generated structures for a single dimer system. We applied this methodology to one of the most challenging molecular cluster systems, namely, the phenyl acetylene (PHA) dimer. In this system, various types of intermolecular interactions

Received: April 30, 2013

Published: July 10, 2013

contribute to and compete in the relative energy order of the dimer geometries.

Phenylacetylene (PHA) is in itself an interesting molecule, in that the benzene ring is not perturbed by any heteroatoms and only mildly perturbed by the weakly electron-withdrawing ethynyl group. The ethynyl group extending the  $\pi$ -system leads to a higher molecular polarizability compared to benzene.<sup>50</sup> The phenylacetylene molecule has three sites available for intermolecular interaction: The  $\pi$  cloud of the benzene ring and the acetylinic  $\text{C}\equiv\text{C}$ , which are both hydrogen bond acceptors, and the acetylinic CH group, which can act as a hydrogen bond donor. These three hydrogen bonding sites allow a competition between  $\pi$ - $\pi$ ,  $\text{CH}\cdots\pi$  and  $\text{CH}\cdots\text{CH}$  interactions. A previous experimental and CCSD(T) study<sup>51</sup> showed that, of these possible binding motifs, the  $\pi$ - $\pi$  interaction was favored by approximately 4 kJ mol<sup>-1</sup> over  $\text{CH}\cdots\pi$  structures but that the variation in  $\pi$ - $\pi$  binding energies was very similar, also about 4 kJ mol<sup>-1</sup>. The shallowness of the potential, regarding these interactions, thus requires “subchemical accuracy”. Dispersion-augmented DFT has been shown to have superior performance over MP2 for the S22 test set of dispersion-bound and  $\pi$ -stacked systems<sup>52</sup> and this “chameleon” system thus represents a unique test for dispersion-augmented and/or van der Waals DFT (vdW DFT).

As the stability of different phenylacetylene dimer geometries is determined by both  $\text{CH}\cdots\pi$  and  $\pi$ - $\pi$  interactions, in varying ratios, a method that correctly predicts the relative stability of PHA dimers must be able to accurately account for both types of interaction. To ensure that this is indeed the case, and to rule out fortuitous error cancellation, the benzene dimer, benzene-methane, and methane dimer were also evaluated using the CCSD(T)/CBS reference geometries of Sherrill et al.<sup>44</sup>

In this paper, we re-investigate the potential energy surface (PES) of the phenylacetylene dimer using several empirical methods, beginning with a stochastic search of the PES using dispersion-augmented third order SCC-DFTB (DFTB3-D<sup>53</sup>) as approximate dispersion-augmented DFT method, then for the lowest energy geometries, benchmark the performance of several semi-empirical density functionals with LC-BOP + van der Waals interaction (LC+vdW) methods<sup>54,55</sup> against perturbation wave function methods.

## ■ COMPUTATIONAL DETAILS

Phenylacetylene dimer geometries were initially determined using the “Kick-fragment”<sup>56</sup> method at the third-order<sup>53</sup> self-consistent<sup>57</sup> charge density functional tight-binding level including dispersion contributions (DFTB3-D)<sup>58</sup> and DFTB parameters from the mio-0-1 parameter set. The seven lowest phenylacetylene dimer geometries, PHA2-(A–G), were optimized by the second-order Møller–Plesset perturbation (MP2) method with cc-pVTZ basis set in previous work,<sup>51</sup> and these refined geometries are employed in this work along with the reference coupled-cluster singles and doubles and perturbative triples (CCSD(T)) energies at the complete-basis-set (CBS) limit. Binding energies, including correction for basis-set superposition error, were computed using four semi-empirical functionals incorporating dispersion effects, B97-D,<sup>12</sup> M05-2x,<sup>59</sup> M06-2x,<sup>45</sup> MPWB1K,<sup>60</sup> and two vdW DFT functionals combining LC-BOP (Becke 1988 exchange<sup>61</sup> + one-parameter progressive correlation functional<sup>62</sup>) with Andersson–Lundqvist (ALL)<sup>63</sup> and local response dispersion (LRD)<sup>64</sup> functionals. The long-range correction (LC)<sup>65</sup> contains an adjustable parameter,  $\mu$ , which determines the

ratio of DFT to HF exchange at intermediate  $r_{12}$ . Tsuneda and co-workers optimized this parameter, giving it a value of 0.33,<sup>66</sup> which is original and now accepted as the optimum for response properties, and 0.47,<sup>67</sup> which is re-optimized to be more appropriate for ground state properties. In this work, we employ and compare both parameter values. The reference calculations<sup>51</sup> employ the aug-cc-pVTZ basis set<sup>68,69</sup> as the largest basis set used to extrapolate to the basis set limit, and so, we adopt this basis set as our “large” basis set. We also employ a triple- $\zeta$  Pople-type basis, 6-311G(d,p).<sup>70</sup> In addition to the density functional methods, MP2 wave function methods were tested, MP2, spin-component-scaled (SCS)-MP2, resolution-of-identity (RI)-MP2 and RI-SCS-MP2, because these are often assumed to give accurate dispersion interactions. All DFT calculations were undertaken using the Gaussian09 program package,<sup>71</sup> and MP2-type calculations employed the TURBO-MOLE program package.<sup>72</sup> The results will be discussed in three sections: dispersion corrected density functional methods, long-range corrected density functional methods, and MP2-type methods.

Finally, a reaction path interconverting the lowest and highest  $\pi$ -stacked PHA2 dimers was calculated using quasi-synchronous transit (QST) calculations. The best-performing of the standard functionals, M06-2x, was used to locate the path and confirm the nature of each stationary point, followed by a single-point energy calculation using LC-BOP+LRD ( $\mu = 0.47$ ). Calculations with both functionals employed the 6-311G(d,p) basis set.

## ■ RESULTS AND DISCUSSION

### Approximate DFT-Based Stochastic Structure Search.

In order to determine the minimum geometry of the PHA dimer and to explore the Potential Energy Surface (PES) of the dimer, random PHA dimers were generated by “Kicking”<sup>56</sup> two PHA molecules. 100 optimizations yielded 21 energetically unique geometries (to  $1 \times 10^{-5}$  a.u.). Inspection of the geometries found only 19 of these to be structurally unique. A further 100 optimizations did not yield any new structures. The energies and  $\Delta E$  with respect to the lowest energy structure of all 19 unique structures are shown in Table 1, binding energies are calculated using the monomer energy of  $-15.95128$  Ha.

It is readily apparent from Table 1 that three different structural motifs or “classes” of structure exist. The lowest energy group, with binding energies falling in a narrow range from  $-27.6$  to  $-24.9$  kJ mol<sup>-1</sup> are all  $\pi$ -stacked structures. Significantly higher in energy, with binding energies ranging from  $-15.5$  to  $-10.1$  kJ mol<sup>-1</sup> are structures where the dimer interaction is of a  $\text{CH}\cdots\pi$  nature, and finally, a small handful of structures, with BEs close to zero, were identified. In this latter group of structures the closest approach of the two monomers was over 4.5 Å. These structures were considered an artifact of the box size used in Kick and not considered any further.

The seven lowest energy structures, including all 5  $\pi$ -stacked dimers and the lowest two  $\text{CH}\cdots\pi$  dimers were selected for further study. MP2/cc-pVTZ re-optimization of these geometries led to the seven previously reported PHA2 geometries.<sup>51</sup> Using these geometries, we performed additional single point binding energy calculations at various vdW DFT, DFT-D, and *ab initio* levels of theory.

**Isomers of the Phenylacetylene Dimer and Relative Stabilities. Molecular Structures.** As the nature of the noncovalent interactions is expected to influence the error in the binding energy, it is useful to first discuss the dimer

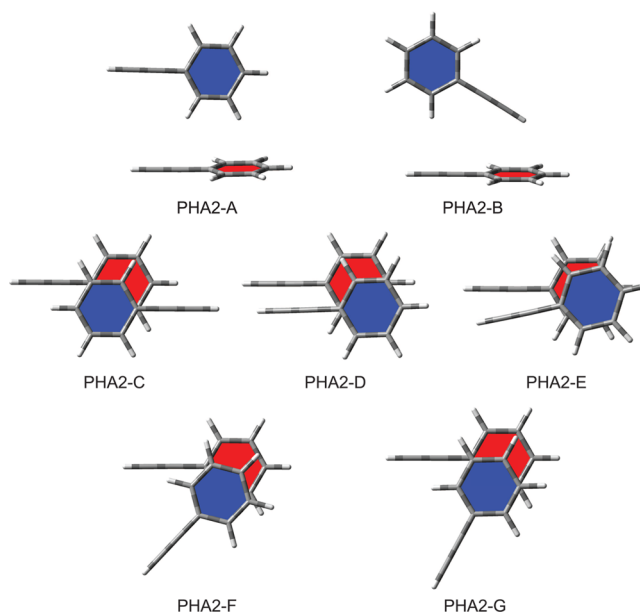
**Table 1.** Kick-Optimized Unique Structures for PHA Dimers Obtained at the DFTB3-D Level of Theory<sup>a</sup>

<i>E</i> (Ha)	$\Delta E$ (eV)	BE (kJ mol <sup>-1</sup> )	structure label
-31.90262	0.284	-0.11	
-31.90264	0.284	-0.16	
-31.90280	0.279	-0.58	
-31.90284	0.278	-0.69	
-31.90300	0.274	-1.11	
-31.90642	0.181	-10.09	
-31.90644	0.180	-10.14	
-31.90700	0.165	-11.61	
-31.90716	0.161	-12.03	
-31.90785	0.142	-13.84	
-31.90805	0.137	-14.37	
-31.90836	0.128	-15.18	
-31.90838	0.128	-15.23	PHA2-B
-31.90848	0.125	-15.50	PHA2-A
-31.91205	0.028	-24.87	PHA2-E
-31.91208	0.027	-24.95	PHA2-D
-31.91228	0.021	-25.47	PHA2-F
-31.91267	0.011	-26.50	PHA2-G
-31.91307	0.000	-27.55	PHA2-C

<sup>a</sup>Structure labels in the final column are consistent with those in ref 51.

structures. Cartesian coordinates and figures of all geometries are included in the Supporting Information. Two general types of binding moiety are represented by PHA2-(A–G). Structures PHA2-A and PHA2-B are both bound by two CH $\cdots\pi$  interactions, differing in the relative orientation of the two PHA units. PHA2-A is a “head-to-head” structure and PHA2-B is a “head-to-tail” dimer. Structures PHA2-(C–G) are all  $\pi$ -stacked dimers that differ in the relative orientation of the acetyl “tails” and the degree of slip between the two monomers: PHA2-C is an anti-parallel structure; PHA2-D has both PHA molecules parallel but slipped; PHA2-E and PHA2-F both have a relative PHA orientation of  $\approx 15^\circ$  but differ in the direction of the slip; Finally, PHA2-G has the PHA molecules at a relative angle of  $\approx 60^\circ$ . PHA2-B, PHA2-C, and PHA2-G are minima, while, at the MP2/cc-pVTZ level, all other structures are transition states.<sup>51</sup> Structures are shown below in Figure 1. The nature of the interactions for the different isomers has been described previously.<sup>51</sup>

**Performance of Popular DFT Methods for Binding Energies.** Table 2 shows the errors in computed binding energies of popular DFT methods relative to the CCSD(T)/CBS energies and the Mean Absolute Deviation (MAD) of the errors calculated for the CH $\cdots\pi$  bound dimers (PHA2-A,B), the  $\pi$ -stacked dimers (PHA2-(C–G)), and the entire set. Sherrill et al. calculated interactions of the benzene and methane dimers using M05-2x and M06-2x, along with several other dispersion-augmented density functionals.<sup>44</sup> Our values, using the CCSD(T)/CBS geometries, replicate theirs closely, with minor differences due to small changes in the geometry. All four semi-empirical functionals tend to underestimate the binding energy probably due to their incomplete dispersion effects. Overall, M06-2x and B97-D are the best performing functionals, with MAD values of 0.8 and 2.0 kJ mol<sup>-1</sup> and 2.4 and 1.5 kJ mol<sup>-1</sup> respectively, using the 6-311G(d,p) and aug-cc-pVTZ basis sets. M05-2x and MPWB1K both severely underestimate the binding energy, with MPWB1K predicting the sandwich benzene dimer (S), parallel-displaced benzene-

**Figure 1.** Reference phenylacetylene dimer minima and transition states (geometries optimized using MP2/cc-pVTZ) from ref 51.

dimer (PD) and PHA2-(D–F) to be unbound. All these functionals exhibit different error behavior for the CH $\cdots\pi$ -bound dimers compared to the  $\pi$ -stacked dimers, with errors in CH $\cdots\pi$  binding energies being approximately half the errors of the  $\pi$ -stacked dimers for the same functional and basis set. M06-2x is the only functional that exhibits the opposite behavior, predicting the binding energy of the  $\pi$ -stacked PHA dimers more accurately than the CH $\cdots\pi$ -bound dimers, though its prediction of the benzene sandwich and parallel-displaced dimers is worse than the benzene–methane and methane–methane dimers, which are in error by less than 1.0 kJ mol<sup>-1</sup>. For the 6-311G(d,p) basis set, the binding energies of the  $\pi$ -stacked dimers are predicted almost exactly, with a MAD of 0.3 kJ mol<sup>-1</sup>, in contrast, the binding energy of both CH $\cdots\pi$ -bound dimers is underestimated by 2.0 kJ mol<sup>-1</sup>. Employing the larger, correlation-consistent basis set increases the MAD to 3.3 and 2.0 kJ mol<sup>-1</sup> for the CH $\cdots\pi$ -bound and  $\pi$ -stacked dimers respectively. The errors for the B97-D functional are less systematic, with the binding energies of PHA2-A being predicted almost exactly for both basis sets and the binding energy of PHA2-F being conspicuously underestimated. B97-D is the sole functional of the four to improve with use of the aug-cc-pVTZ basis set and this is due to lower errors for the  $\pi$ -stacked dimers. The benzene and methane dimers are predicted almost exactly with this combination. It should be noted that both of these functionals yield errors that are below the typical 4 kJ/mol<sup>-1</sup> (1 kcal/mol<sup>-1</sup>) threshold for “chemical accuracy”.

**Performance of LC+vdW Methods for Binding Energies.** Errors in computed binding energies, with respect to the CCSD(T)/CBS binding energies, are presented for the LC-BOP functional in Tables 3 and 4. The first two columns show the LC-BOP functional with the ALL dispersion correction applied (i.e., LC-BOP+ALL),<sup>63</sup> and second two columns show the errors when LRD correction<sup>64,73</sup> is applied (i.e., LC-BOP+LRD).

Employing the lower value of  $\mu$  results in most binding energies being slightly overestimated for both the benzene and methane dimer combinations and the PHA dimers. The ALL dispersion correction performs somewhat better than the LRD

**Table 2. Errors (kJ mol<sup>-1</sup>) in BSSE Corrected Binding Energies Relative to CCSD(T)/CBS for Dimer Complexes Calculated Using Several Density Functionals<sup>a</sup>**

	B97-D		M05-2x		M06-2x		MPWB1K		CCSD(T)
	6-311G(d,p)	aug-cc-pVTZ	6-311G(d,p)	aug-cc-pVTZ	6-311G(d,p)	aug-cc-pVTZ	6-311G(d,p)	aug-cc-pVTZ	CBS
S	-1.2	0.2	-6.2	-5.9	-3.8	-4.5	-11.7	-11.5	6.9
T	0.4	0.2	-2.8	-3.1	-1.6	-2.3	-6.4	-7.1	11.3
PD	-1.2	0.0	-4.5	-5.0	-1.1	-2.1	-12.3	-13.3	11.2
CH <sub>4</sub> -benzene	-0.3	-0.3	-1.1	-1.5	-0.2	-0.8	-3.0	-3.6	6.2
CH <sub>4</sub> -CH <sub>4</sub>	-0.2	0.0	-0.1	-0.2	-0.2	-0.6	-1.5	-1.6	2.3
PHA2-A	0.3	-0.1	-4.6	-5.5	-2.0	-3.2	-9.6	-11.1	15.6
PHA2-B	-1.5	-1.7	-4.6	-5.6	-2.0	-3.4	-9.8	-11.3	14.8
PHA2-C	-2.4	-1.8	-7.6	-9.4	0.0	-2.0	-18.2	-20.7	21.2
PHA2-D	-2.6	-1.8	-8.0	-9.8	-0.1	-2.4	-17.6	-20.0	17.3
PHA2-E	-2.7	-1.7	-7.8	-9.5	-0.1	-2.3	-17.3	-19.7	17.7
PHA2-F	-3.7	-3.0	-9.4	-8.1	0.3	-1.9	-19.9	-22.4	17.8
PHA2-G	-0.9	-0.4	-6.4	-11.3	0.7	-1.4	-15.4	-17.7	17.9
MAD (A-B)	0.9	0.9	4.6	5.5	2.0	3.3	9.7	11.2	
MAD (C-G)	2.5	1.7	7.8	9.6	0.3	2.0	17.7	20.1	
MAD	2.0	1.5	6.9	8.5	0.8	2.4	15.4	17.5	

<sup>a</sup>“S”, “T”, and “PD” refer to the sandwich, T-shaped, and parallel displaced isomers of the benzene dimer, respectively. Benzene and methane CCSD(T)/CBS results taken from ref 44; phenylacetylene CCSD(T)/CBS binding energies ( $-\Delta E$ ) are taken from ref 51.

**Table 3. Errors (kJ mol<sup>-1</sup>) in BSSE Corrected Binding Energies Relative to CCSD(T)/CBS for Dimer Complexes Calculated Using LC-BOP+ALL and LC-BOP+LRD Density Functionals with the HF Mixing Parameter  $\mu = 0.33^a$** 

	LC-BOP+ALL		LC-BOP+LRD		CCSD(T)
	6-311G(d,p)	aug-cc-pVTZ	6-311G(d,p)	aug-cc-pVTZ	CBS
S	3.2	4.0	0.5	0.9	6.9
T	2.8	3.2	1.6	1.2	11.3
PD	2.2	2.4	2.3	2.3	11.2
CH <sub>4</sub> -benzene	2.8	2.7	1.7	1.3	6.2
CH <sub>4</sub> -CH <sub>4</sub>	2.0	2.0	1.0	0.9	2.3
PHA2-A	2.6	3.0	2.5	1.7	15.6
PHA2-B	2.0	2.0	3.0	2.2	14.8
PHA2-C	-0.5	-0.4	4.9	4.1	21.2
PHA2-D	0.3	0.3	4.7	3.9	17.3
PHA2-E	0.3	0.4	4.8	4.0	17.7
PHA2-F	-2.3	-2.4	3.5	2.6	17.8
PHA2-G	1.3	1.2	5.2	4.3	17.9
MAD (A-B)	2.3	2.5	2.8	2.0	
MAD (C-G)	1.1	1.2	4.3	3.5	
MAD	1.3	1.4	4.1	3.3	

<sup>a</sup>“S”, “T”, and “PD” refer to the sandwich, T-shaped, and parallel displaced isomers of the benzene dimer, respectively. Benzene and methane CCSD(T)/CBS results taken from ref 44; phenylacetylene CCSD(T)/CBS results ( $-\Delta E$ ) are taken from ref 51.

correction, particularly for the five  $\pi$ -stacked dimers, where the MAD is just over 1 kJ mol<sup>-1</sup>, though the binding energies of two dimers, PHA2-C and PHA2-F are underestimated. In contrast, LRD produces worse errors (MAD of 4.3 and 3.5 kJ mol<sup>-1</sup> for the 6-311G(d,p) and aug-cc-pVTZ basis sets, respectively) for the  $\pi$ -stacked PHA dimers. As both functionals and basis sets consistently overestimate the binding energy of the CH $\cdots\pi$ -bound dimers by approximately 2.5 kJ mol<sup>-1</sup>, it is the errors for the  $\pi$ -stacked dimers that dictate the overall difference in MAD for the two functionals. This situation is reversed for the higher value of  $\mu$ , with LRD performing significantly better than ALL. Considering first the benzene and methane dimers, LRD yields a maximum error of 1.0 kJ mol<sup>-1</sup>. Both functional and basis set combinations yield the binding energy of the CH $\cdots\pi$ -bound dimers to within 1 kJ mol<sup>-1</sup>. ALL underestimates the binding energies of the  $\pi$ -stacked dimers by an average of 3.4 and 3.7 kJ mol<sup>-1</sup>. The LRD dispersion

correction provides an overestimate using the 6-311G(d,p) basis, but a slight underestimate when using the aug-cc-pVTZ basis set. With the exception of the binding energy of the PHA2-F transition state structure, which is underestimated in all cases, the LC-BOP+LRD functional provides the most consistent calculation of binding energies, with MAD values all  $\leq 1$  kJ mol<sup>-1</sup>.

**Performance of MP2-Type Methods for Binding Energies.** Previous work<sup>51</sup> compared CCSD(T)/CBS extrapolated binding energies with the MP2/aug-cc-pVDZ and MP2/aug-cc-pVTZ calculations used in the extrapolation. In these, a substantial difference was observed between the binding energies of the CH $\cdots\pi$ -bound dimers and the  $\pi$ -stacked dimer, with the former being overestimated by approximately 4 kJ mol<sup>-1</sup> and the latter being overestimated by approximately 14 kJ mol<sup>-1</sup>. In this work, the performance of the RI- and SCS-modifications to MP2 is shown in Table 5. Employing the RI



**Table 4.** Errors ( $\text{kJ mol}^{-1}$ ) in BSSE Corrected Binding Energies Relative to CCSD(T)/CBS for Dimer Complexes Calculated Using LC-BOP+ALL and LC-BOP+LRD Density Functionals with the HF Mixing Parameter  $\mu = 0.47^a$ 

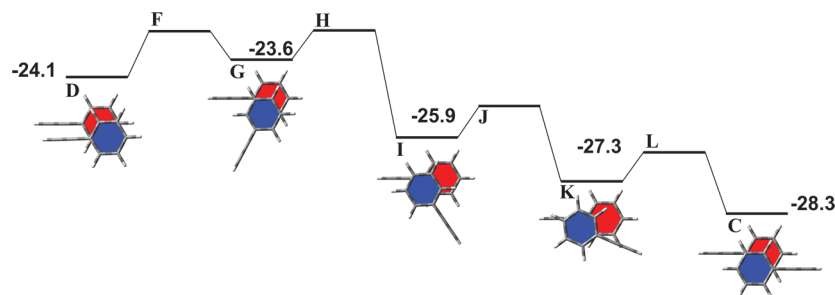
	LC-BOP+ALL		LC-BOP+LRD		CCSD(T)
	6-311G(d,p)	aug-cc-pVTZ	6-311G(d,p)	aug-cc-pVTZ	CBS
S	1.4	2.6	−1.0	−0.8	6.9
T	1.5	1.9	0.3	−0.1	11.3
PD	−0.2	0.2	0.1	−0.1	11.2
CH <sub>4</sub> –benzene	1.8	1.5	0.7	0.3	6.2
CH <sub>4</sub> –CH <sub>4</sub>	1.5	1.5	0.6	0.4	2.3
PHA2-A	0.5	0.8	0.4	−0.4	15.6
PHA2-B	−0.2	−0.2	0.7	−0.2	14.8
PHA2-C	−4.5	−4.8	0.8	−0.4	21.2
PHA2-D	−3.5	−3.8	0.7	−0.5	17.3
PHA2-E	−3.4	−3.6	0.9	−0.3	17.7
PHA2-F	−6.6	−7.1	−1.0	−2.4	17.8
PHA2-G	−2.1	−2.5	1.6	0.4	17.9
MAD (A–B)	0.4	0.5	0.6	0.3	
MAD (C–G)	3.4	3.7	1.0	0.7	
MAD	3.0	3.3	0.9	0.7	

<sup>a</sup>“S”, “T”, and “PD” refer to the sandwich, T-shaped, and parallel displaced isomers of the benzene dimer, respectively. Benzene and methane CCSD(T)/CBS results taken from ref 44; phenylacetylene CCSD(T)/CBS results ( $-\Delta E$ ) are taken from ref 51.

**Table 5.** Errors in BSSE Corrected Binding Energies ( $\text{kJ mol}^{-1}$ ) Relative to CCSD(T)/CBS for Dimer Complexes Calculated Using RI- and SCS-MP2 Methods<sup>a</sup>

	MP2	SCS-MP2	RI-MP2	RI-SCS-MP2	CCSD(T)
	6-311G(d,p)	6-311G(d,p)	aug-cc-pVTZ	aug-cc-pVTZ	CBS
S	−1.4	−5.3	5.9	0.5	6.9
T	−2.4	−5.7	2.8	−1.5	11.3
PD	−2.0	−7.4	7.4	0.1	11.2
CH <sub>4</sub> –benzene	−2.6	−4.4	1.1	−1.5	6.2
CH <sub>4</sub> –CH <sub>4</sub>	−1.9	−2.3	−0.3	−1.1	2.3
PHA2-A	−3.1	−8.4	4.7	−2.1	15.6
PHA2-B	−4.3	−9.4	4.6	−2.3	14.8
PHA2-C	−2.6	−13.0	13.2	−0.4	21.2
PHA2-D	−2.3	−11.9	13.1	0.3	17.3
PHA2-E	−2.2	−11.7	13.1	0.3	17.7
PHA2-F	−3.6	−14.4	13.1	−1.2	17.8
PHA2-G	−1.2	−10.3	12.5	0.5	17.9
MAD (A–B)	3.7	8.9	4.6	2.2	
MAD (C–G)	2.4	12.2	13.0	0.6	
MAD	2.8	11.3	10.6	1.0	

<sup>a</sup>Benzene and methane CCSD(T)/CBS results taken from ref 44; phenylacetylene CCSD(T)/CBS results ( $-\Delta E$ ) are taken from ref 51.

**Figure 2.** Stationary points on the phenylacetylene dimer potential energy surface showing the rotation between parallel-displaced (PHA2-D) and anti-parallel-displaced (PHA2-C) structures. Binding energies, in  $\text{kJ mol}^{-1}$  are electronic energy only and are with respect to the separated PHA monomers.

approximation requires the availability of an optimized auxiliary basis and is therefore currently not applicable to the MP2/6-311G(d,p) level of theory. The RI-approximation using the

aug-cc-pVTZ basis set however does not improve the situation significantly relative to non-RI MP2, with  $\text{CH}\cdots\pi$ -bound dimers still overestimated by  $\approx 4 \text{ kJ mol}^{-1}$ , but the  $\pi$ -stacked dimers

now being overestimated by  $\approx 13 \text{ kJ mol}^{-1}$ . Additionally, using SCS (RI-SCS-MP2) results in  $\text{CH}\cdots\pi$ -bound dimers now being underestimated by  $\approx 2 \text{ kJ mol}^{-1}$  while the  $\pi$ -stacked dimer BEs (S, PD, PHA2-(C-G)) are predicted almost exactly, with errors less than  $\pm 0.5 \text{ kJ mol}^{-1}$ . The only exception is isomer PHA2-F, which is underestimated by  $1.2 \text{ kJ mol}^{-1}$ .

**Rotational Potential Energy Profile of PHA2.** It is apparent that the  $\pi$ -stacked structures, being bound only by dispersion forces and covering a narrow range of energy (only  $4.2 \text{ kJ mol}^{-1}$ ), could feasibly interconvert. The reaction path connects PHA2-D, where the two PHA units are positioned parallel but displaced, to the lowest energy dimer, PHA2-C (anti-parallel displaced). This pathway is shown in Figure 2, and Table 6 gives the binding energies for both the M06-2x and LC-BOP+LRD functionals.

**Table 6. Reaction Path Linking PHA2-D (Parallel, Displaced) and PHA2-C (Anti-parallel, Displaced) Structures<sup>a</sup>**

structure	no. imaginary frequencies	M06-2x BE ( $\text{kJ mol}^{-1}$ )	LC-BOP+LRD BE ( $\text{kJ mol}^{-1}$ )
PHA2-D	0	-24.1	-25.0
PHA2-F	1	-22.7	-25.2
PHA2-G	0	-23.6	-25.9
PHA2-H	1	-22.7	-25.4
PHA2-I	0	-25.9	-27.3
PHA2-J	1	-25.0	-27.4
PHA2-K	0	-27.3	-28.4
PHA2-L	1	-26.4	-28.7
PHA2-C	0	-28.3	-29.1

<sup>a</sup>Structure labels A–G in the first column are consistent with those in ref 51.

As expected, given that both ends of the pathway are within “chemical accuracy” ( $1 \text{ kcal mol}^{-1}$ ) of each other, the rearrangement is facile, with the largest barrier in the forward direction (PHA2-D  $\rightarrow$  PHA2-C) being only  $1.4 \text{ kJ mol}^{-1}$  and  $3.2 \text{ kJ mol}^{-1}$  in the reverse direction. Even the zero-point energy provides sufficient energy to surmount sub-kJ  $\text{mol}^{-1}$  barriers, and thus, the conversion of PHA2-D to PHA2-C is effectively barrierless. Such a barrierless rearrangement is consistent with previous reports that showed that temperatures below  $\approx 115 \text{ K}$  were needed to stabilize the phenylacetylene dimer.<sup>51</sup>

## CONCLUSIONS

A stochastic search based on dispersion-augmented approximate DFT was used to systematically search isomers of the phenylacetylene dimer (PHA2). Binding energies with respect to the monomer were calculated using dispersion corrected DFT, semi-empirical and LC+vdW functionals, and several MP2 methods for low energy  $\pi$ -stacked and  $\text{CH}\cdots\pi$  isomers of the phenylacetylene dimer. All MP2 methods and most density functionals were found to yield different errors for  $\pi$ -stacked and  $\text{CH}\cdots\pi$  structures, highlighted by the benzene and methane dimers; however, the LC-BOP+LRD functional yielded sub-kJ  $\text{mol}^{-1}$  barriers for all structures, regardless of the basis set employed. It is thereby demonstrated that a combination of DFTB3-D-based Kick stochastic search and LC-BOP-based vdW DFT binding energy calculations is capable to perform coupled cluster quality predictions for molecular cluster complex geometries and their energies. Our prediction of a reaction pathway converting parallel and anti-parallel  $\pi$ -stacked

structures is in agreement with the weak nature of the intermolecular interaction in the PHA2 system.

## ASSOCIATED CONTENT

### Supporting Information

MP2/cc-pVTZ optimized geometries of all reference structures, all Kick-located minima, and the full reaction pathway for the conversion of PHA2-D to PHA2-C. This material is available free of charge via the Internet at <http://pubs.acs.org>.

## AUTHOR INFORMATION

### Corresponding Author

\*E-mail: [sirle@chem.nagoya-u.ac.jp](mailto:sirle@chem.nagoya-u.ac.jp)

### Present Address

<sup>||</sup>School of Engineering and Science, Jacobs University Bremen, Campus Ring 1, 28759 Bremen, Germany

### Notes

The authors declare no competing financial interest.

## ACKNOWLEDGMENTS

Calculations were performed at the Institute for Molecular Science (IMS) in Okazaki, Japan. We also thank the XSEDE program for generous computer time at NICS, Oak Ridge National Lab. M.A.A. acknowledges the JSPS Fellowship Program and travel support from a EU seventh Framework Marie Curie Actions IRSES project (grant no: 295172). This work was also supported by the Japanese Ministry of Education, Culture, Sports, Science, and Technology (MEXT) (Grants: 23225001 and 24350005) and by a CREST (Core Research for Evolutional Science and Technology) grant on the synthesis and novel functions of soft  $\pi$ -materials from the Japanese Science and Technology Agency (JST).

## REFERENCES

- Uyeda, C.; Jacobsen, E. N. *J. Am. Chem. Soc.* **2011**, *133*, 5062–5075.
- Crittenden, D. L. *J. Phys. Chem. A* **2009**, *113*, 1663–1669.
- Marshall, M. S.; Burns, L. A.; Sherrill, C. D. *J. Chem. Phys.* **2011**, *135*, 194102.
- Zhang, Y.; Hollman, D. S.; Schaeffer, H. F. I. *J. Chem. Phys.* **2012**, *136*, 244305.
- Quiñonero, D.; Estarellas, C.; Frontera, A.; Deyà, P. M. *Chem. Phys. Lett.* **2011**, *508*, 144–148.
- Tsuzuki, S. *ChemPhysChem* **2012**, *13*, 1664–1670.
- Adcock, S. A.; McCammon, J. A. *Chem. Rev.* **2006**, *106*, 1589–1615.
- Huenerbein, R.; Schirmer, B.; Moellmann, J.; Grimme, S. *Phys. Chem. Chem. Phys.* **2010**, *12*, 6940–6948.
- Klimes, J.; Michaelides, A. *J. Chem. Phys.* **2012**, *137*, 120901.
- Grimme, S. *J. Comput. Chem.* **2004**, *25*, 1463–1473.
- Becke, A. D.; Johnson, E. R. *J. Chem. Phys.* **2007**, *127*, 154108.
- Grimme, S. *J. Comput. Chem.* **2006**, *27*, 1787–1799.
- Grimme, S.; Antony, J.; Ehrlich, S.; Krieg, H. *J. Chem. Phys.* **2010**, *132*, 154104.
- Gruneis, A.; Marsman, M.; Harl, J.; Schimka, L.; Kresse, G. *J. Chem. Phys.* **2009**, *131*, 154115.
- Krishtal, A.; Vanommeslaeghe, K.; Olasz, A.; Veszpremi, T.; Alsenoy, C. V.; Geerlings, P. *J. Chem. Phys.* **2009**, *130*, 174101.
- Toulouse, J.; Zhu, W.; Savin, A.; Jansen, G.; Angyan, J. G. *J. Chem. Phys.* **2011**, *135*, 084119.
- Janesko, B. G.; Henderson, T. M.; Scuseria, G. E. *J. Chem. Phys.* **2009**, *130*, 081105.
- Bludsky, O.; Rubes, M.; Soldan, P.; Nachtigall, P. *J. Chem. Phys.* **2008**, *128*, 114102.

- (19) Steinmann, S. N.; Corminboeuf, C. *J. Chem. Phys.* **2011**, *134*, 044117.
- (20) Vydrov, O. A.; Voorhis, T. V. *J. Chem. Phys.* **2010**, *133*, 244103.
- (21) von Lilienfeld, O. A.; Tkatchenko, A. *J. Chem. Phys.* **2010**, *132*, 234109.
- (22) Hesselmann, A. *J. Chem. Phys.* **2009**, *130*, 084104.
- (23) Vydrov, O. A.; Voorhis, T. V. *J. Chem. Phys.* **2009**, *130*, 104105.
- (24) Chai, J.-D.; Head-Gordon, M. *J. Chem. Phys.* **2009**, *131*, 174105.
- (25) Ambrosetti, A.; Silvestrelli, P. L. *Phys. Rev. B* **2012**, *85*, 073101.
- (26) Chermak, E.; Mussard, B.; Ángyán, J.; Reinhardt, P. *Chem. Phys. Lett.* **2012**, *550*, 162–169.
- (27) Raju, R. K.; Bloom, J. W. G.; An, Y.; Wheeler, S. E. *ChemPhysChem* **2011**, *12*, 3116–3130.
- (28) Goerigk, L.; Kruse, H.; Grimme, S. *ChemPhysChem* **2011**, *12*, 3421–3433.
- (29) Granatier, J.; Pitoňák, M.; Hobza, P. *J. Chem. Theory Comput.* **2012**, *8*, 2282–2292.
- (30) Ershova, O. V.; Besley, N. A. *J. Chem. Phys.* **2012**, *136*, 244313.
- (31) Fedorov, I.; Zhuravlev, Y.; Berveno, V. *Phys. Status Solidi B* **2012**, *249*, 1438–1444.
- (32) Frayret, C.; Izgorodina, E. I.; MacFarlane, D. R.; Villesuzanne, A.; Barres, A.-L.; Politano, O.; Rebeix, D.; Poizot, P. *Phys. Chem. Chem. Phys.* **2012**, *14*, 11398–11412.
- (33) Mishra, B. K.; Karthikeyan, S.; Ramanathan, V. *J. Chem. Theory Comput.* **2012**, *8*, 1935–1942.
- (34) Vydrov, O. A.; Van Voorhis, T. *J. Chem. Theory Comput.* **2012**, *8*, 1929–1934.
- (35) da Costa, L. M.; Stoyanov, S. R.; Gusarov, S.; Tan, X.; Gray, M. R.; Stryker, J. M.; Tykewinski, R.; de M. Carneiro, J. W.; Seidl, P. R.; Kovalenko, A. *Energy Fuels* **2012**, *26*, 2727–2735.
- (36) Janowski, T.; Pulay, P. *Chem. Phys. Lett.* **2007**, *447*, 27–32.
- (37) Sinnokrot, M. O.; Sherrill, C. D. *J. Phys. Chem. A* **2006**, *110*, 10656–10668.
- (38) Sinnokrot, M. O.; Valeev, E. F.; Sherrill, C. D. *J. Am. Chem. Soc.* **2002**, *124*, 10887–10893.
- (39) Lee, E. C.; Kim, D.; Jurečka, P.; Tarakeshwar, P.; Hobza, P.; Kim, K. S. *J. Phys. Chem. A* **2007**, *111*, 3446–3457.
- (40) Janowski, T.; Pulay, P. *J. Am. Chem. Soc.* **2012**, *134*, 17520–17525.
- (41) Pitoňák, M.; Neogrády, P.; Řezáč, J.; Jurečka, P.; Urban, M.; Hobza, P. *J. Chem. Theory Comput.* **2008**, *4*, 1829–1834.
- (42) Zhao, Y.; Truhlar, D. G. *J. Phys. Chem. A* **2005**, *109*, 4209–4212.
- (43) Jurečka, P.; Černý, J.; Hobza, P.; Salahub, D. R. *J. Comput. Chem.* **2007**, *28*, 555–569.
- (44) Sherrill, C. D.; Takatani, T.; Hohenstein, E. G. *J. Phys. Chem. A* **2009**, *113*, 10146–10159.
- (45) Zhao, Y.; Truhlar, D. *Theor. Chem. Acc.* **2008**, *120*, 215–241.
- (46) Takatani, T.; Hohenstein, E. G.; Malagoli, M.; Marshall, M. S.; Sherrill, C. D. *J. Chem. Phys.* **2010**, *132*, 144104.
- (47) Podeszwa, R.; Patkowski, K.; Szalewicz, K. *Phys. Chem. Chem. Phys.* **2010**, *12*, 5974–5979.
- (48) Tao, J.; Perdew, J. P.; Staroverov, V. N.; Scuseria, G. E. *Phys. Rev. Lett.* **2003**, *91*, 146401.
- (49) Riley, K. E.; Pitoňák, M.; Černý, J.; Hobza, P. *J. Chem. Theory Comput.* **2010**, *6*, 66–80.
- (50) Lucas, X.; Quiñonero, D.; Frontera, A.; Deyà, P. M. *J. Chem. Phys. A* **2009**, *113*, 10367–10375.
- (51) Maity, S.; Patwari, G. N.; Addicoat, M. A.; Irle, S.; Sedlak, R.; Hobza, P. *Phys. Chem. Chem. Phys.* **2011**, *13*, 21651–21652.
- (52) Tsuneda, T.; Taketsugu, T. In  *$\pi$ -Stacked Polymers and Molecules*; Nakano, T., Ed.; Springer: New York, 2013.
- (53) Gaus, M.; Cui, Q.; Elstner, M. *J. Chem. Theory Comput.* **2011**, *7*, 931–948.
- (54) Kamiya, M.; Tsuneda, T.; Hirao, K. *J. Chem. Phys.* **2002**, *117*, 6010–6015.
- (55) Sato, T.; Tsuneda, T.; Hirao, K. *J. Chem. Phys.* **2007**, *126*, 234114.
- (56) Addicoat, M.; Metha, G. *J. Comput. Chem.* **2009**, *30*, 57–64.
- (57) Elstner, M.; Porezag, D.; Jungnickel, G.; Elsner, J.; Haugk, M.; Frauenheim, T.; Suhai, S.; Seifert, G. *Phys. Rev. B* **1998**, *58*, 7260–7268.
- (58) Elstner, M.; Hobza, P.; Frauenheim, T.; Suhai, S.; Kaxiras, E. *J. Chem. Phys.* **2001**, *114*, 5149–5155.
- (59) Zhao, Y.; Schultz, N.; Truhlar, D. *J. Chem. Theory Comput.* **2006**, *2*, 364–382.
- (60) Zhao, Y.; Truhlar, D. *J. Chem. Phys. A* **2004**, *108*, 6908–6918.
- (61) Becke, A. *J. Chem. Phys.* **1988**, *38*, 3098–3100.
- (62) Tsuneda, T.; Suzumura, T.; Hirao, K. *J. Chem. Phys.* **1999**, *110*, 10664–10678.
- (63) Andersson, Y.; Langreth, D. C.; Lundqvist, B. I. *Phys. Rev. Lett.* **1996**, *76*, 102–105.
- (64) Sato, T.; Nakai, H. *J. Chem. Phys.* **2010**, *133*, 194101.
- (65) Iikura, H.; Tsuneda, T.; Yanai, T.; Hirao, K. *J. Chem. Phys.* **2001**, *115*, 3540–3544.
- (66) Tawada, Y.; Tsuneda, T.; Yanagisawa, S.; Yanai, T.; Hirao, K. *J. Chem. Phys.* **2004**, *120*, 8425–8433.
- (67) Song, J.-W.; Hirose, T.; Tsuneda, T.; Hirao, K. *J. Chem. Phys.* **2007**, *126*, 154105.
- (68) Dunning, T., Jr. *J. Chem. Phys.* **1989**, *90*, 1007.
- (69) Kendall, R.; Dunning, T., Jr.; Harrison, R. *J. Chem. Phys.* **1992**, *96*, 6796.
- (70) Krishnan, R.; Binkley, J. S.; Seeger, R.; Pople, J. A. *J. Chem. Phys.* **1980**, *72*, 650–654.
- (71) Frisch, M. J.; Trucks, G. W.; Schlegel, H. B.; Scuseria, G. E.; Robb, M. A.; Cheeseman, J. R.; Scalmani, G.; Barone, V.; Mennucci, B.; Petersson, G. A.; Nakatsuji, H.; Caricato, M.; Li, X.; Hratchian, H. P.; Izmaylov, A. F.; Bloino, J.; Zheng, G.; Sonnenberg, J. L.; Hada, M.; Ehara, M.; Toyota, K.; Fukuda, R.; Hasegawa, J.; Ishida, M.; Nakajima, T.; Honda, Y.; Kitao, O.; Nakai, H.; Vreven, T.; Montgomery, Jr., J. A.; Peralta, J. E.; Ogliaro, F.; Bearpark, M.; Heyd, J. J.; Brothers, E.; Kudin, K. N.; Staroverov, V. N.; Kobayashi, R.; Normand, J.; Raghavachari, K.; Rendell, A.; Burant, J. C.; Iyengar, S. S.; Tomasi, J.; Cossi, M.; Rega, N.; Millam, J. M.; Klene, M.; Knox, J. E.; Cross, J. B.; Bakken, V.; Adamo, C.; Jaramillo, J.; Gomperts, R.; Stratmann, R. E.; Yazyev, O.; Austin, A. J.; Cammi, R.; Pomelli, C.; Ochterski, J. W.; Martin, R. L.; Morokuma, K.; Zakrzewski, V. G.; Voth, G. A.; Salvador, P.; Dannenberg, J. J.; Dapprich, S.; Daniels, A. D.; Farkas, Á.; Foresman, J. B.; Ortiz, J. V.; Cioslowski, J.; Fox, D. J. *Gaussian 09 Revision B.1*; Gaussian Inc.: Wallingford, CT, 2009.
- (72) *TURBOMOLE V6.3 2011*, a development of University of Karlsruhe and Forschungszentrum Karlsruhe GmbH, 1989–2007, TURBOMOLE GmbH, since 2007; available from <http://www.turbomole.com>.
- (73) Ikabata, Y.; Sato, T.; Nakai, H. *Int. J. Quantum Chem.* **2012**, DOI: 10.1002/qua.24092.